Bioresource Technology 416 (2025) 131755

Contents lists available at ScienceDirect

Bioresource Technology

journal homepage: www.elsevier.com/locate/biortech

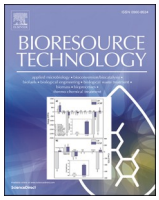

Engineering thermotolerant *Kluyveromyces marxianus* strains for resveratrol production by simultaneous saccharification and fermentation of whole slurry corn cob

Marlene Baptista [a], Carlos E. Costa [a,b], Lucília Domingues [a,b,*]

[a] Centre of Biological Engineering, University of Minho, Campus Gualtar, 4710-057 Braga, Portugal
[b] LABBELS –Associate Laboratory, Braga/Guimarães, Portugal

HIGHLIGHTS

- *Kluyveromyces marxianus* efficiently produces *p*-coumaric acid and its derivatives.
- Resveratrol production by *K. marxianus* was reported for the first time.
- Xylose fermentation leads to higher resveratrol titres than glucose.
- Ethanol supplementation favoured resveratrol production from xylose.
- High resveratrol titre was attained from a corn cob hydrolysate and whole slurry.

ARTICLE INFO

Keywords:
Resveratrol
p-Coumaric acid
Kluyveromyces marxianus
Corn cob
Whole slurry

ABSTRACT

The microbial biosynthesis of the antioxidant compound resveratrol offers an eco-friendly and sustainable alternative to chemical synthesis or plant extraction. Here, we showed that *Kluyveromyces marxianus* strains produce *p*-coumaric acid, a key precursor of resveratrol, with higher titres achieved under increased agitation conditions. Through further strain engineering, resveratrol production was achieved using glucose, xylose, and/or ethanol as substrates. Xylose emerged as the most favourable carbon source for resveratrol production, with ethanol supplementation during xylose culture resulting in increased resveratrol titres by limiting the accumulation of the by-product xylitol. At 37 ∘C, resveratrol production from corn cob hydrolysate and whole slurry substantially increased the yield of resveratrol per sugar, reaching titres of up to 69.26 mg/L. This work shows, for the first time, resveratrol production by *K. marxianus* and from corn cob whole slurry, establishing foundations for the development of an integrated sustainable process for resveratrol production from lignocellulosic materials.

1. Introduction

Industrial interest in producing naturally occurring plant secondary metabolites, such as resveratrol, is growing at a fast pace. This compound has proven antioxidant, anti-inflammatory, and anti-ageing activities, which make it appealing to the pharmaceutical and cosmetic industries (De La Lastra and Villegas, 2005). The most common method for its obtention is chemical extraction from plants, usually grape skins, and seeds, the leaves of Japanese giant knotweed, among others, in a process dependent on plant availability that results in low yield and purity (Donnez et al., 2009). Resveratrol can also be obtained by chemical synthesis at relatively high yields. Nonetheless, this process has a high environmental impact and lacks stereoselectivity, resulting in the production of *cis*-resveratrol, which is not responsible for the main biological functions (Solladié et al., 2003). On the other hand, microbial production of resveratrol has been emerging as an environmentally and economically sustainable alternative (Costa et al., 2024) that enables the precise obtention of the *trans*-isomer of this compound. *De novo* production of resveratrol has been reported in different hosts, such as the bacteria *Escherichia coli* (Kang et al., 2014) and the yeast *Scheffersomyces stipitis* (Kobayashi et al., 2021), *Saccharomyces cerevisiae* (Li et al., 2016), and *Yarrowia lypolytica* (Gu et al., 2020; Sáez-Sáez et al., 2020).

* Corresponding author at: Centre of Biological Engineering, University of Minho, Campus Gualtar, 4710-057 Braga, Portugal.
E-mail address: luciliad@deb.uminho.pt (L. Domingues).

https://doi.org/10.1016/j.biortech.2024.131755
Received 29 May 2024; Received in revised form 25 October 2024; Accepted 5 November 2024
Available online 5 November 2024
0960-8524/© 2024 The Author(s). Published by Elsevier Ltd. This is an open access article under the CC BY license (http://creativecommons.org/licenses/by/4.0/).

Resveratrol production by these microorganisms has been achieved by introducing heterologous plant genes that use the aromatic amino acids tyrosine and/or phenylalanine, produced via the shikimate pathway.

The generation of low-value wastes, shortage of resources, and climate change experienced worldwide have prompted a paradigm shift from linear to circular economies. The goal of the latest is to increase the speed at which low-value renewable substrates, such as lignocellulosic materials, are recovered, recycled, and/or valorised to obtain high-value products. Lignocellulosic materials, which are the most abundant feedstock and are globally available, typically consist of 30–60 % (on a dry basis) of cellulose, 20–40 % of hemicellulose, and 10–25 % of lignin. Among these materials, corn cob—an agricultural by-product generated in large quantities worldwide from maize processing—has emerged as a promising feedstock for biorefineries. Its potential lies in its abundant availability and substantial xylan content (Gandam et al., 2022). Breaking down the recalcitrant structure of lignocellulosic biomass through a pretreatment allows the recovery of each component either in solid or liquid fractions, thereby enhancing the accessibility of carbohydrates for subsequent enzymatic hydrolysis. Among many available pretreatment (Shafiei-Alavijeh et al., 2024), autohydrolysis is advantageous since it uses hot water, no toxic solvents, and low energy during the process. Besides, depending on the severity factor, it is possible to have a compromise between the solubilisation of polymers from hemicellulose (i.e, xylooligosaccharides) and the concentration of inhibitory compounds generated (e.g., acetic acid, furfural, 5-hydroxymethylfurfural, and phenolic compounds). Following autohydrolysis, the solid phase (cellulosic fraction) can be used to obtain glucose through enzymatic saccharification, while the liquid phase (hemicellulosic fraction) can be subjected to hydrolysis to obtain xylose. The mixture of the liquid and solid phases, called whole slurry, improves fermentation by increasing sugar concentration, compared to the separate fractions, avoids additional time constraints and separation costs, and the excessive use of water, thereby reducing sugars dilution (del Río et al., 2019). Simultaneous Saccharification and Fermentation (SSF) process configuration allows the combination of enzymatic hydrolysis and fermentation to produce desired compounds in a single step, thereby reducing the process costs, sugar inhibition, and risk of contamination compared to separate hydrolysis and fermentation (SHF) (Baptista et al., 2018). The use of a thermotolerant microorganism, such as the non-conventional yeast *Kluyveromyces marxianus* would be desirable for this type of process since this yeast can withstand near-optimal saccharification temperatures (Baptista and Domingues, 2022), thereby increasing the saccharification yield and reducing cooling costs for the fermentation step.

The yeast *K. marxianus* has been emerging as an alternative cell factory to produce ethanol, high-value chemicals, and heterologous enzymes with a wide range of applications in the food, feed, and pharmaceutical industries (Karim et al., 2020). The current research interest in *K. marxianus* is attributed to its unique features, such as high growth rate when compared to other eukaryotes, thermotolerance, tolerance to low pH (Madeira-Jr and Gombert, 2018), and the capacity to metabolise a broad range of sugar substrates (lactose, glucose, xylose, inulin, fructose, arabinose, galactose, among others) (Lane and Morrissey, 2010). Therefore, the utilisation of *K. marxianus* in biorefineries is increasingly gaining traction, primarily because of its capacity to metabolise diverse inexpensive feedstocks derived from agro-industrial activities (Baptista and Domingues, 2022). Compared to Crabtree-positive yeast, like *S. cerevisiae*, the Crabtree-negative metabolism of *K. marxianus* may be advantageous to produce resveratrol since its metabolism is diverted from ethanol production to other metabolites, such as acetyl-CoA (Sakihama et al., 2019). The potential of *K. marxianus* to produce aromatic compounds, such as 2-phenylethanol, through the shikimate pathway was previously highlighted after metabolic engineering to increase the supply of phosphoenolpyruvate (PEP) and erythrose-4-phosphate (E4P) to this pathway (Li et al., 2021). Strains of *K. marxianus* exhibit heterogeneity regarding osmotolerance, thermotolerance, ethanol tolerance, and capacity to resist cell wall-damaging agents (Lane and Morrissey, 2010), which highlights the importance of selecting the appropriate chassis strain for the desired process (Costa et al., 2017). In the case of lignocellulosic-based processes, strains capable of simultaneously withstanding inhibitors (Baptista et al., 2021) and consuming several sugars without repression at high temperatures are essential to develop an integrated process.

In this study, two *K. marxianus* strains, one laboratory strain and one isolate from Brazilian cocoa fermentation, were engineered for the first time to produce resveratrol through the tyrosine pathway using glucose, xylose and/or ethanol as carbon sources. The recombinant strains were then successfully utilised as hosts for resveratrol production from pretreated corn cob hydrolysate and whole slurry by SSF at 37 ∘C, establishing grounds for the development of an integrated sustainable process for high-value resveratrol production from lignocellulosic materials.

2. Materials and methods

2.1. Corn cob

Corn cob, harvested locally at a farm in Braga, in the North of Portugal, was used as a raw material in fermentation experiments. Corn cob elemental composition was as follows: 0.02 ± 0.01 mg of nitrogen (0.43 ± 0.05 %), 1.40 ± 0.07 mg of carbon (42.41 ± 2.24 %), 0.22 ± 0.02 mg of hydrogen (6.45 ± 0.37 %).

2.2. Media

E. coli transformants were selected and maintained on Lysogeny Broth (LB) plates (1 % NaCl, 1 % peptone, 0.5 % yeast extract, and 1.5 % agar) with the appropriate antibiotic (100 g/L ampicillin, 50 g/L kanamycin or 50 g/L chloramphenicol). Yeast strains were kept in YPD plates (1 % yeast extract, 2 % peptone, 2 % dextrose, 1.5 % agar). YPD plates with 200 g/L hygromycin B were used for yeast transformation. Fermentation experiments were performed in YPD_{20} (1 % yeast extract, 2 % peptone, 2 % dextrose) or YPX_{20} (1 % yeast extract, 2 % peptone, 2 % xylose) unless specified otherwise.

2.3. Construction of plasmids and strains

Cloning procedures were done using *E. coli* NZY5α competent cells (NZYTech). Plasmid construction was made by Golden Gate using YTK parts (Addgene) (Lee et al., 2015; Weber et al., 2011) and some parts from the *Kluyveromyces* Kit according to the protocols by Rajkumar et al., 2019. Plasmids provided by others were the following: p2584 (Li et al., 2016), pGGKd015 (Hassing et al., 2019), pGGKd072 (Hassing et al., 2021), and pGGkd068 (Dekker et al., 2021); the remaining were built in-house. Confirmation of correct gene cloning into the YTK entry vector (pYTK001) was done by Sanger sequencing (Eurofins genomics) and confirmation of other plasmids assembly was done by colony PCR using NZYTaq II 2x Green Master Mix (NZYTech) and by restriction digestion with *Not*I followed by analysis in agarose gel.

Yeast transformation was done following the LiOAc/PEG method (Gietz, 2014). Successful single integrations into the *lac4* locus were confirmed by PCR using NZYLong 2x Green Master Mix (NZYTech). This locus was selected because previous studies (Rajkumar et al., 2019) demonstrated it is an optimal integration site, offering efficiency and stable insertions that do not interfere with core metabolism. One *K. marxianus* strain previously isolated from cocoa fermentation, named S9, (Pereira et al., 1999) and the laboratory strain YBL001 derived from NBRC1777 with inactivated non-homologous end-joining mechanism (*yku80-1*) (Rajkumar et al., 2019) were used in this work. Strain S9 was selected considering that previous research by the authors revealed that it can be used at 37 ∘C advantageously (Baptista et al., 2021). To construct strains S9-*FjTAL* and YBL001-*FjTAL* expressing the tyrosine ammonia lyase coding gene from *Flavobacterium johnsoniae* (*FjTAL*) for

evaluation of *p*-coumaric acid production, the *FjTAL* gene from pCfB8373, codon optimised for expression in *S. cerevisiae* (Li et al., 2016), was initially cloned into pYTK001 via *Bsm*BI Golden Gate reaction. The *FjTAL* gene under the control of native *PDC1* promoter and *S. cerevisiae ADH1* terminator was cloned into pGGKd015 via *Bsa*I Golden Gate reaction, originating plasmid pUDE-*FjTAL*. mVenus gene from pYTK033 was cloned into pGGKd072 under the control of the same promoter and terminator, as a fluorescent reporter. Both gene expression cassettes were cloned into pGGKd068 via *Bsm*BI Golden Gate reaction to originate MB-pUDI-002. Additionally, to construct S9-RBP and YBL001-RBP strains harbouring a resveratrol biosynthetic pathway (RBP) composed of *FjTAL*, *p*-coumaroyl-CoA ligase (*At4CL2*) from *Arabidopsis thaliana* and resveratrol synthase (*VvVST1*) from *Vitis vinifera*, *At4CL2* and *VvVST1* from p2584, codon optimised for expression in *S. cerevisiae* (Li et al., 2016), were initially cloned into pYTK001 via *Bsm*BI Golden Gate reaction. pGGKd123 plasmid used to clone gene expression cassettes was built by *Bsa*I Golden Gate reaction using pYTK095, pYTK003, pYTK047, and pYTK068, while pGGKd124 was built using pYTK095, pYTK004, pYTK047, and pYTK072. The *At4CL2* gene under the control of native *PDC1* promoter and *INU1* terminator was cloned into pGGKd123 via *Bsa*I Golden Gate reaction, originating plasmid pGGKd123-*At4CL2*, while *VvVST1* under the control of the native *TEF1* promoter and *PDC1* terminator was cloned into pGGKd124, originating plasmid pGGKd124-*VvVST1*. The three gene expression cassettes were cloned into pGGKd068 via *Bsm*BI Golden Gate reaction to originate MB-pUDI-003. Both MB-pUDI-002 and MB-pUDI-003 were digested with *Not*I before yeast transformation with 2 μg and 4 μg of each cassette for YBL001 and S9 strains, respectively.

2.4. Fermentation experiments

Depending on the assay, precultures of yeast cells were done overnight in 50 mL shake flasks with a working volume of 10 mL of YPD_{20} or YPX_{20} with 300 rpm orbital shaking at 30 ∘C. All fermentation assays were carried out in an orbital shaker at 300 rpm unless specified otherwise, and 30 ∘C, with biological duplicates or triplicates. In all fermentations, a ratio of culture volume to flask volume was kept at 1:5. The content of sugars, glycerol, xylitol, acetic acid, and ethanol was monitored by the collection of a 500 μL supernatant sample. Another 500 μL sample was mixed with the same volume of ethanol (>99 % purity), vortexed for 10 s, and the supernatant collected after centrifugation was analysed for *p*-coumaric acid and resveratrol quantification (Costa et al., 2021).

The production of *p*-coumaric acid was evaluated in YPD medium in shake flasks at 200 rpm and baffled shake flasks at 300 rpm, to evaluate the agitation effect, and in YPD or YPX in baffled shake flasks and 96-deep-well plates at 300 rpm, to compare the production from glucose and xylose. For all the assays, the initial $OD_{600\ nm}$ was 0.1. *De novo* resveratrol production was assessed in YPD medium in 50 mL cultures, as well as the influence of yeast extract concentration and peptone supplementation on both resveratrol and biomass production. The effect of increasing glucose concentration (36, 105, and 170 g/L) on resveratrol production was also assessed. Additionally, resveratrol production from xylose, with or without ethanol supplementation (5 g/L pulses at 12 and 24 h), was investigated. For all experiments, the initial inoculum was set at an $OD_{600\ nm}$ of 1.

2.5. Resveratrol production from corn cob hydrolysate and whole slurry by SSF

Resveratrol production from the hemicellulosic fraction of hydrothermally pretreated corn cob was evaluated in 100 mL shake flasks at 37 ∘C, supplemented with 1 % yeast extract and 2 % peptone. This temperature was selected because *K. marxianus* is thermotolerant, and strain S9 has been shown to grow well at 37 ∘C (Baptista et al., 2021). Using temperatures in SSF that are close to the optimal enzyme temperature is crucial for enhancing hydrolysis efficiency. Cells were precultured in YPX_{20}, given that xylose was the predominant readily available sugar in the hemicellulosic hydrolysate. They were then recovered by centrifugation (5 min, 3000*xg*) and resuspended in sterile water to achieve an inoculum concentration of 8 mg of fresh yeast per mL. Resveratrol production was evaluated by SSF of the whole slurry of hydrothermally pretreated corn cob using a 5 % solid loading and 12 FPU of cellulase per gram of autohydrolysed corn cob. Cellic CTec2, kindly provided by Novozymes (Bagsvaerd, Denmark), had an activity of 122 FPU mL^{-1}, measured by the method described by (Ghose, 1987). Fermentation conditions were the same as those used for the hydrolysate.

2.6. Pretreatment of corn cob

Corn cob was milled and subjected to autohydrolysis using a liquid-to-solid ratio (LSR) of 8 kg of water per kg of dried corn cob residue in a 2 L pressurised Parr reactor. The process was conducted in a non-isothermal regime at 205 ∘C, corresponding to a severity of 3.85, according to previous optimisations for this residue (Rivas et al., 2006). The elemental composition of the corn cob solid fraction was as follows: 0.01 ± 0.00 mg of nitrogen (0.24 ± 0.04 %), 1.53 ± 0.09 mg of carbon (44.14 ± 0.50 %), 0.22 ± 0.02 mg of hydrogen (6.24 ± 0.10 %).

After pretreatment, the solid and liquid phases were separated by filtration. The solid phase was sterilized at 121 °C for 20 min, while the liquid phase underwent a second step of acid hydrolysis with 0.5 % (w/w) H_2SO_4 for 165 min at 125 °C (Rivas et al., 2006). The corn cob solid fraction was analysed for chemical composition following a standard NREL protocol (NREL/TP-510-42618-42622-4218). The hydrothermally pretreated corn cob solid composition was (measured as g per 100 g of pretreated corn cob on an oven dry basis ± standard deviation): 35.95 ± 1.54 % of glucan, 17.41 ± 0.41 % of xylan, and 15.70 ± 1.20 % of Klason lignin. The obtained hydrolysate was neutralized with $CaCO_3$ until it reached a pH of 5.05 and detoxified with activated charcoal at a ratio of 1 g of activated charcoal per 10 g of hydrolysate for 1 h with agitation at room temperature. This step aimed to reduce the phenolics content present in the hydrolysate, which was previously reported to hinder resveratrol detection by UHPLC (Costa et al., 2022a). The activated charcoal was removed by filtration, and the hydrolysate was subsequently sterilised by filtration through a 0.22 μm pore filter. The composition of the detoxified corn cob hydrolysate measured by HPLC was as follows: 21.13 ± 0.01 g/L xylose, 1.70 ± 0.23 g/L glucose, 3.57 ± 0.02 g/L arabinose, and 3.05 ± 0.12 g/L acetic acid. The hydrolysate contained 5.52 ± 0.01 mg/L of *p*-coumaric acid, while the whole slurry contained 22.96 ± 0.12 mg/L.

2.7. Analytical methods

Fermentation samples were analysed for glucose, xylose, glycerol, acetic acid, and ethanol concentration by HPLC using a BioRad Aminex HPX-87H column, at 60 ∘C, with a mobile phase of 5 mM H_2SO_4 and flow rate of 0.6 mL min^{-1}. Peaks were detected using a refractive index detector. Resveratrol and *p*-coumaric acid were quantified by UHPLC equipped with a Discovery HS F5 150 mm × 2.1 mm column (particle size 3 mm). The eluent flow rate was 0.7 mL min^{-1}, using a linear gradient from 5 % to 60 % of acetonitrile over 10 mM ammonium formate (pH 3.0, adjusted with formic acid) from 0.5 − 9.5 min. Resveratrol and *p*-coumaric acid were detected by absorbance at 333 nm with retention times of 5.5 and 4.4 min, respectively (Costa et al., 2022a).

The $OD_{600\ nm}$ was measured using a GeneQuant 100 spectrophotometer (GE Healthcare). Biomass dry cell weight was quantified by collecting 1 mL of fermentation broth in previously dried and weighted tubes. The pellet was washed with ethanol to remove any resveratrol or *p*-coumaric acid, then with deionized water, incubated at 105 ∘C for 24 h, and weighted again.

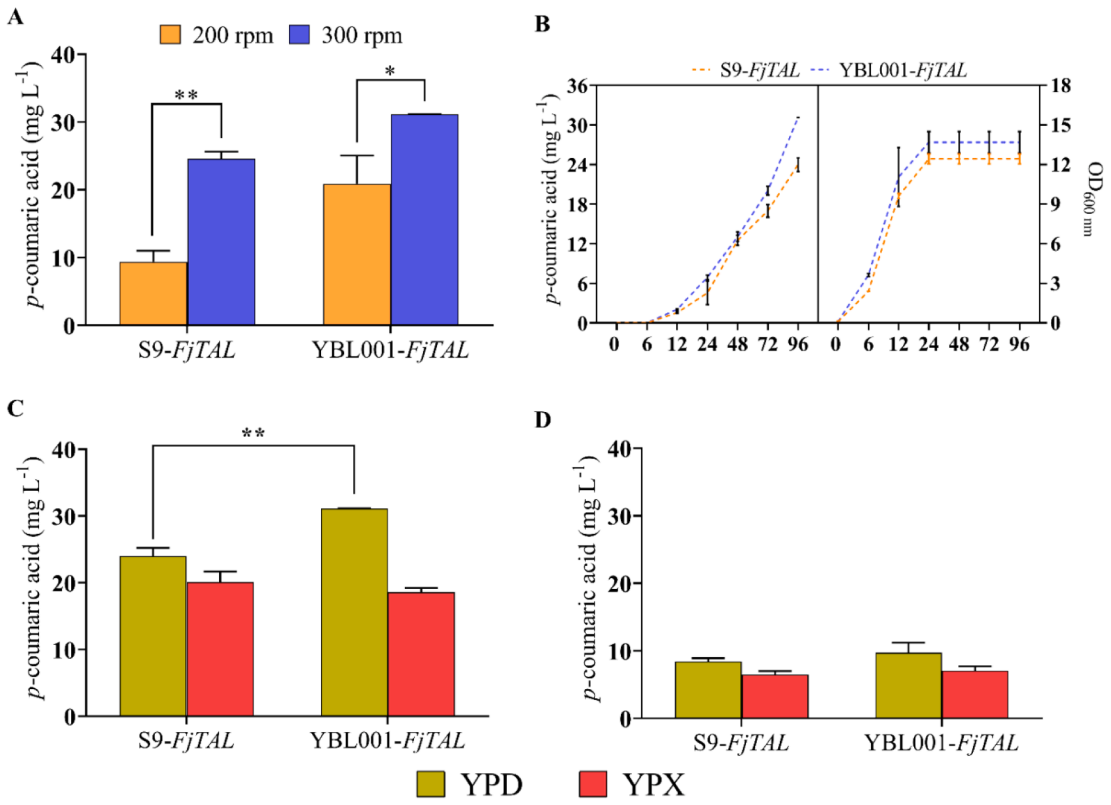

Fig. 1. *p*-coumaric acid production under different conditions. End-point (96 h) *p*-coumaric acid concentration produced at 30 ∘C at 200 (orange) and 300 (blue) rpm in YPD medium by S9-*FjTAL* and YBL001-*FjTAL* (A). Time course of *p*-coumaric acid concentration and $OD_{600\ nm}$ by S9-*FjTAL* (orange line) and YBL001-*FjTAL* (blue line) and (B) end-point (96 h) *p*-coumaric acid concentration in YPD (green) or YPX medium (pink) for fermentations in baffled shake flasks (C) or 96-deep-well plates (D) at 30 ∘C and 300 rpm. Each data point represents the average ± standard deviation of biological triplicates.

Elemental analysis of corn cob (untreated) and hydrothermally pretreated corn cob solid (treated) was performed using a UNICUBE elemental analyser (Elementar), according to the 5 mg standard method in duplicates. The amount of untreated and treated samples used was 3.30 ± 0.00 mg and 3.45 ± 0.15 mg, respectively.

2.8. Statistical analysis

Statistical analyses were conducted using GraphPad Prism for Windows version 8.0.2, using two-way ANOVA and the Tukey *post hoc* test. Statistical significance was considered at a p value < 0.05, with "ns" denoting nonsignificant results (p value > 0.05), * indicating p value < 0.05, ** denoting p value < 0.01, *** indicating p value < 0.001, and **** denoting p value < 0.0001.

3. Results and discussion

3.1. Engineering K. marxianus to produce resveratrol precursor: p-coumaric acid

Resveratrol production results from the reaction of *p*-coumaroyl-CoA with malonyl-CoA in a stoichiometric ratio of 1:3 (Vos et al., 2015). In this work, we introduced the gene coding for a tyrosine ammonia lyase from *Flavobacterium johnsoniae* (*FjTAL*) into the *K. marxianus lac4* locus, which catalyses the deamination of tyrosine into *p*-coumaric acid. Both S9-*FjTAL* and YBL001-*FjTAL* strains were transformed with 100 % efficiency from the colonies tested and produced *p*-coumaric acid from glucose, with significantly higher yields (2.6-fold higher for S9-*FjTAL* and 1.5-fold for YBL001-*FjTAL*) under increased agitation (300 vs 200 rpm) (Fig. 1A). Increased agitation likely enhances oxygen transfer rates, influencing the overall metabolism and secondary metabolite biosynthesis (Furukawa et al., 1983). Additionally, higher aeration reduces alcoholic fermentation, diverting pyruvate to the tricarboxylic acid (TCA) cycle. Interestingly, at 300 rpm, *p*-coumaric acid accumulation continued exponentially even during the stationary growth phase (Fig. 1B). Although $OD_{600\ nm}$ did not increase from 24 to 96 h, the increased *p*-coumaric accumulation during this period may result from its export to the extracellular space. This is a toxic compound and the exportation phenomenon occurs as a mechanism to reduce its toxicity (Mao et al., 2023). The production of *p*-coumaric acid from glucose was significantly higher than from xylose for both strains (S9-*FjTAL*, p value < 0.05; YBL001-*FjTAL*, p value < 0.001) in baffled shake flasks (Fig. 1C). Strain YBL001-*FjTAL* performed better in YPD medium (achieving 31.12 ± 0.02 mg/L), but no significant differences were observed between the strains for the production from xylose (Fig. 1A and C). The higher production of *p*-coumaric acid from glucose compared to xylose may be attributed to the fact that one of its key precursors, PEP, is generated through glycolysis (Sakihama et al., 2019), the primary metabolic pathway for glucose under aerobic conditions. In contrast, xylose is metabolised via the pentose phosphate pathway (PPP), which generates E4P, another precursor of *p*-coumaric acid (Fig. 2A). Therefore, it can be hypothesised that during xylose metabolism, lower levels of PEP are produced, leading to reduced *p*-coumaric acid synthesis compared to glucose. Interestingly, engineered *S. cerevisiae* strains that metabolise xylose through the xylose reductase/xylitol dehydrogenase (XR/XDH) pathway produced 45 times more *p*-coumaric acid from xylose than from glucose due to reduced overflow metabolism(Borja et al., 2019). The final concentration of *p*-coumaric acid from xylose or glucose in 96-deep-well plates was approximately three times lower than in baffled shake flasks at 300 rpm for both strains. No significant differences were observed between the strains under the same conditions (YPD or YPX) in the 96-deep-well plates (Fig. 1D). The lower production observed in 96-

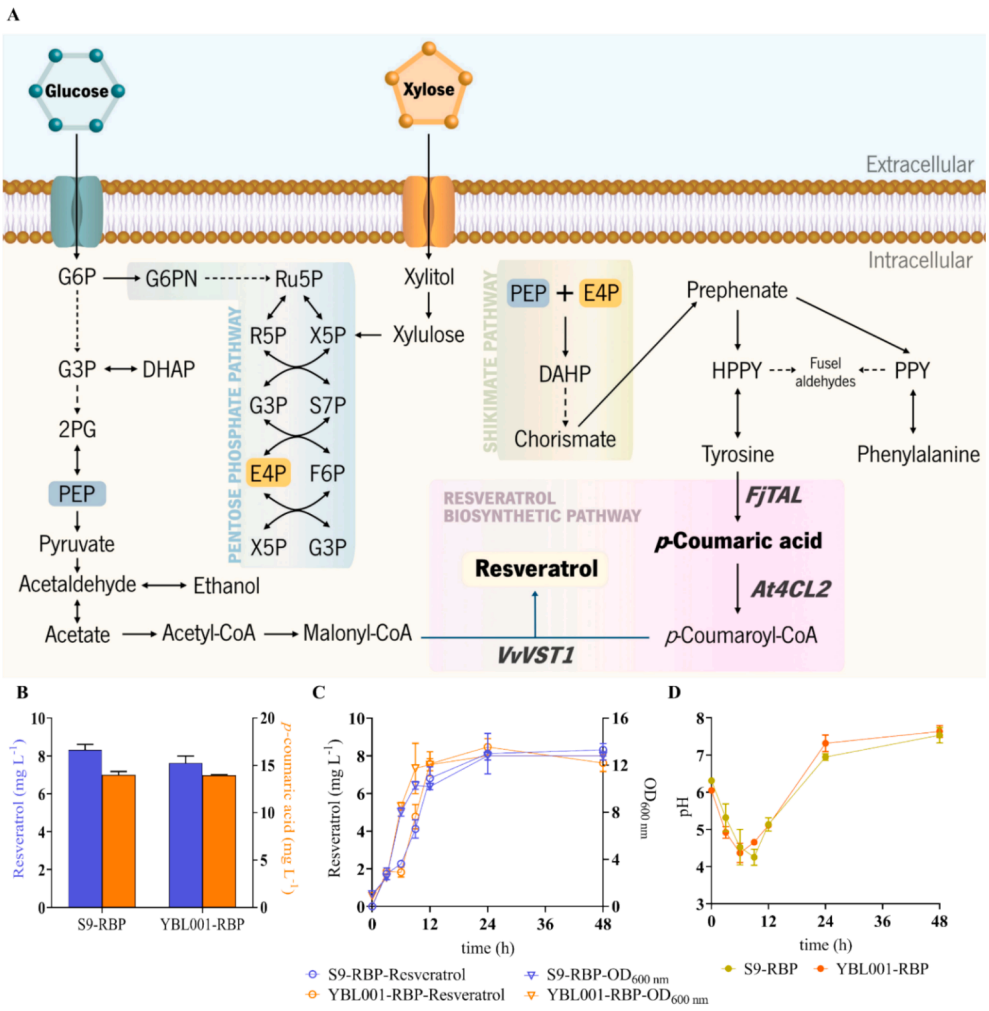

Fig. 2. Resveratrol production from glucose. (A) Metabolic context involved in the *de novo* resveratrol biosynthesis by the two engineered yeast strains expressing the resveratrol biosynthetic pathway (RBP), S9-RBP and YBL001-RBP. Full arrows represent single reaction steps in either direction, and dashed arrows represent multiple reaction steps. Genes of the Resveratrol Biosynthetic Pathway (RBP) are presented in bold grey (*FjTAL*, *At4CL2*, and *VvVST1*). Abbreviations: G6P, glucose 6-phosphate; F6P, fructose 6-phosphate; F16BP, fructose 1,6-bisphosphate; DHAP, dihydroxyacetone phosphate; G3P, glyceraldehyde 3-phosphate; 2PG, 2-phosphoglycerate; PEP, 2-phosphoenolpyruvate; G6PN, 6-phosphogluconolactone; Ru5P, ribulose-5-phosphate; R5P, ribose-5-phosphate; X5P, xylulose-5-phosphate; S7P, sedoheptulose-7-phosphate; E4P, erythrose-4-phosphate; DAHP, 3-deoxy-D-arabinoheptulosonate-7-phosphate; HPPY, hydroxyphenylpyruvate; PPY, phenylpyruvate. (B) End-point (48 h) resveratrol (blue bars) and *p*-coumaric acid (orange bars) production. (C) Profile of resveratrol and $OD_{600\ nm}$, and pH (D) by the two engineered yeast strains expressing the resveratrol biosynthetic pathway (RBP), S9-RBP and YBL001-RBP, after 48 h of fermentation in baffled shake flasks in YPD medium at 30 ∘C and 300 rpm. Each column represents the average values ± standard deviation of biological triplicates.

deep-well plates could be due to limited oxygen transfer, negatively impacting biomass formation. Moreover, baffled shake flasks allow for higher oxygen transfer compared to regular shake flasks.

Furthermore, strain S9-*FjTAL* produced 1.1 times more ethanol than strain YBL001-*FjTAL*, with both strains consuming it after 48 h. In the fermentation in baffled shake flasks, glucose was consumed faster (within 9 h) than xylose (after 48 h) by both strains, as expected. The yield of *p*-coumaric acid per biomass dry weight, the yield of *p*-coumaric acid per consumed sugar, and productivity were 1.3-fold significantly higher (p value < 0.0001) for YBL001-*FjTAL* than for S9-*FjTAL* in YPD medium at 96 h. This is consistent with YBL001-*FjTAL* producing 1.3 times more *p*-coumaric acid than S9-*FjTAL*. Also, the yield of *p*-coumaric acid per biomass dry cell weight was significantly higher (p value $<$ 0.0001) for both strains (S9-*FjTAL* – 1.3-fold, YBL001-*FjTAL* – 1.8-fold) in YPD compared to YPX. The yield of *p*-coumaric acid per consumed sugar for YBL001-*FjTAL* was 1.5-fold significantly higher (p value $<$ 0.0001) in YPD compared to YPX. Significantly higher productivity was observed in YPD compared to YPX for both strains (S9-*FjTAL* – 1.2-fold with a p value < 0.005; YBL001-*FjTAL* – 1.7-fold with a p value $<$ 0.0001).

3.2. *De novo* production of resveratrol from glucose by engineered *K. marxianus* strains

After demonstrating the capability of *K. marxianus* strains to produce *p*-coumaric acid, both strains were engineered to express a resveratrol biosynthetic pathway (RBP) through tyrosine (Fig. 2A). This pathway includes three genes: *FjTAL*, *At4CL2*, and *VvVST1*. *At4CL2* catalyses the conversion of *p*-coumaric acid, produced earlier by the action of *FjTAL*, into *p*-coumaroyl-CoA. This reaction requires ATP and involves the formation of *p*-coumarate-AMP as an intermediate, which subsequently binds with coenzyme A to produce *p*-coumaroyl-CoA, releasing AMP in the process. The final enzyme in this pathway, *VvVST1*, condenses three molecules of malonyl-CoA with *p*-coumaroyl-CoA to synthesize resveratrol. *VvVST1* codes for the rate-limiting enzyme of this pathway (Li et al., 2016), and thus, it was expressed under the control of a strong promoter to prevent the accumulation of pathway intermediates. The rationale for the combination of promoters and terminators used to

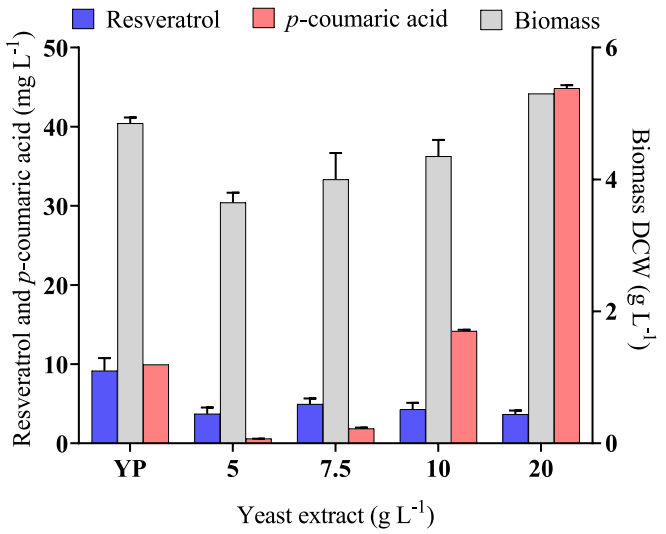

Fig. 3. Optimisation of media supplementation for resveratrol production. Resveratrol (blue bars), *p*-coumaric acid (pink bars), and biomass dry cell weight (DCW; grey bars) concentrations at the end of fermentation (96 h) by strain YBL001-RBP in glucose media supplemented with different concentrations of yeast extract (from 5, 7.5, 10, and 20 g/L) against the control standard YP supplementation (10 g/L of yeast extract and 20 g/L of peptone) at 30 ∘C and 300 rpm. Each column represents the average values ± standard deviation of biological duplicates.

express the RBP was supported by previous work by Rajkumar et al., 2019 and Dekker et al., 2021. This pathway is more compact than the phenylalanine pathway, requiring one less heterologous gene, which may reduce metabolic burden. Although the phenylalanine pathway is reported to be the most efficient for resveratrol production in *S. cerevisiae*, successful application of the tyrosine pathway has also been reported in *S. cerevisiae* (Li et al., 2015) and *Y. lypolytica* (Gu et al., 2020), as well as the combination of both pathways (Sáez-Sáez et al., 2020). *De novo* resveratrol production was first evaluated from glucose at 30 ∘C and 300 rpm (Fig. 2B), as these conditions led to high *p*-coumaric acid accumulation. Additionally, since resveratrol production is highly dependent on ATP formation (Vos et al., 2015), adequate oxygenation of the fermentation media is crucial. Resveratrol production was observed for both strains with no significant differences between them. Resveratrol accumulation showed an exponential increase until 12 h of fermentation, marking the onset of the stationary growth phase (Fig. 2C). Despite the pH being equal to or higher than 7 from 24 h onward, which is known to impact *trans*-resveratrol stability (Robinson et al., 2015), the concentration of resveratrol remained unchanged during that period (Fig. 2D). The accumulation of *p*-coumaric acid was observed for both strains only after 24 h, reaching a final concentration of 14.00 ± 0.35 mg/L for strain S9-RBP and 13.94 ± 0.06 mg/L for YBL001-RBP, which is approximately double the concentration of resveratrol produced by both strains (Fig. 2B). This observed accumulation of *p*-coumaric acid at the end of the fermentation suggests a possible bottleneck downstream in the pathway, potentially due to insufficient malonyl-CoA (Mao et al., 2023). Malonyl-CoA is derived from acetyl-CoA through the action of the enzyme acetyl-CoA carboxylase (Acc1) (Fig. 2A). Strategies to increase malonyl-CoA concentration could simultaneously reduce *p*-coumaric acid accumulation and enhance resveratrol production. One such approach involves replacing the native *ACC1* with a mutant version, as shown in *S. cerevisiae* to increase (*S*)-naringenin production. Additionally, the use of malonyl-CoA biosensors, coupled with this engineering strategy, could help regulate *p*-coumaric acid biosynthesis and optimize malonyl-CoA levels (Mao et al., 2023). From another perspective, increasing the acetyl-CoA pool and the supply of other shikimate pathway precursors, such as E4P and PEP (Fig. 2A), could also increase malonyl-CoA levels. This could be achieved by introducing a heterologous pathway (e.g., phosphoketolase/ phosphotransacetylase pathway) and/or overexpressing of the native *ENO1* gene (Rajkumar and Morrissey, 2020). Moreover, overexpressing multiple copies of genes downstream of *FjTAL* in the resveratrol biosynthetic pathway (*At4CL2* and *VvVST1*) could further mitigate *p*-coumaric acid accumulation. The accumulation of *p*-coumaric acid also reflects the native negative feedback mechanism caused by *Aro3*, *Aro7*, and *Aro4*, which are limited by tyrosine accumulation (Rajkumar and Morrissey, 2020). Glucose was consumed by both strains after 12 h (data not shown), acetic acid was undetected throughout fermentation and no ethanol was detected after 48 h of fermentation. No significant differences were observed between strains on the yield of resveratrol per dry cell weight (S9-RBP – 1.72 ± 0.06 mg g^{-1}, YBL001-RBP – 1.56 ± 0.08 mg g^{-1}), yield of resveratrol per initial glucose concentration (S9-RBP – 0.49 ± 0.02 mg g^{-1}, YBL001- RBP – 0.45 ± 0.02 mg g^{-1}) and productivity (S9- RBP – 0.17 ± 0.01 mg/Lh^{-1},

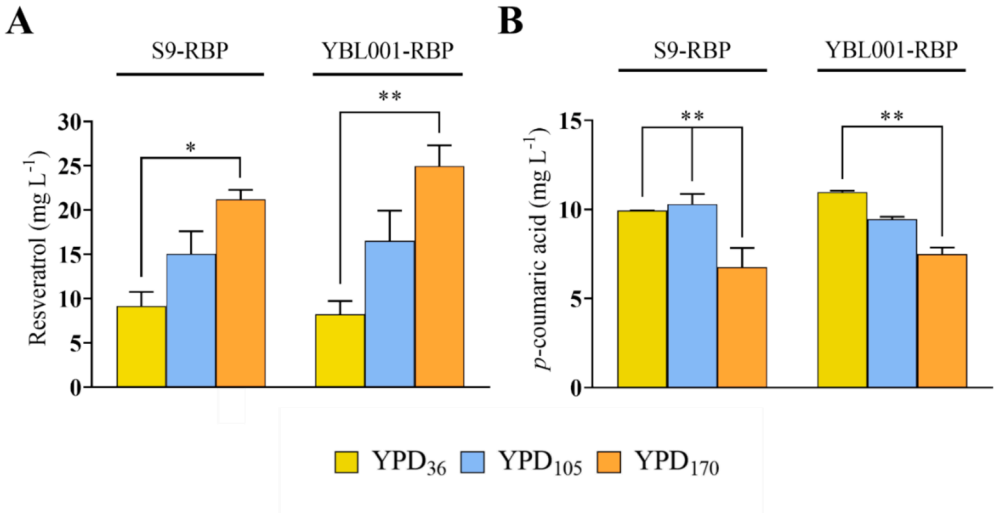

Fig. 4. Effect of increasing glucose concentration on resveratrol production. Resveratrol production (A) and *p*-coumaric acid accumulation (B) by the two engineered yeast expressing the resveratrol biosynthetic pathway (RBP), S9-RBP and YBL001-RBP, after 48 h of fermentation in baffled shake flasks in YPD medium with different glucose concentration (36 (green), 105 (blue), and 170 (orange) g/L) at 30 ∘C and 300 rpm. Each column represents the average values ± standard deviation of biological duplicates.

Table 1
Fermentation parameters of resveratrol production with increasing glucose concentration. Fermentation parameters of the recombinant strains expressing the resveratrol biosynthetic pathway (RBP) in two different host chassis (laboratory strain YBL001 and isolate from cocoa fermentation strain S9) in YPD with 36, 105 and 170 g/L of glucose at 30 ∘C.[a]

Strain	G_0 (g/L)	E_{24h} (g/L)	R_{48h} (mg/L)	DCW_{48h} (g/L)	$Y_{R/DCW-48h}$ (mg g^{-1})	$Y_{R/G-48h}$ (mg g^{-1})	Q_{R-48h} (mg/Lh^{-1})
S9-RBP	36.29 ± 1.71	0.00 ± 0.00	9.16 ± 1.60	4.51 ± 0.15	2.03 ± 0.35	0.25 ± 0.04	0.19 ± 0.03
	105.14 ± 8.20	0.00 ± 0.00	15.06 ± 2.56	5.75 ± 0.09	2.62 ± 0.45	0.14 ± 0.02	0.31 ± 0.05
	169.40 ± 1.49	2.12 ± 0.09	21.21 ± 1.08	6.85 ± 0.45	3.10 ± 0.16	0.13 ± 0.01	0.44 ± 0.02
YBL001-RBP	36.29 ± 1.71	0.00 ± 0.00	8.25 ± 1.49	5.25 ± 0.55	1.57 ± 0.28	0.23 ± 0.04	0.17 ± 0.03
	105.14 ± 8.20	0.00 ± 0.00	16.52 ± 3.42	6.25 ± 0.15	2.64 ± 0.55	0.16 ± 0.03	0.34 ± 0.07
	169.40 ± 1.49	1.78 ± 0.20	24.98 ± 2.33	7.45 ± 0.25	3.35 ± 0.31	0.15 ± 0.01	0.52 ± 0.05

[a] G_0, initial glucose concentration; E_{24h}, ethanol concentration at 24 h; R_{48h}, resveratrol concentration in the end of fermentation (48 h); DCW_{48h}, Dry Cell Weight in the end of fermentation (48 h); $Y_{R/DCW-48h}$, Yield of resveratrol per dry cell weight at 48 h; $Y_{R/G-48h}$, yield of resveratrol at 48 h per glucose concentration consumed; Q_{R-48h}, resveratrol productivity at 48 h.

YBL001-RBP − 0.16 ± 0.01 mg/Lh^{-1}) at 48 h.

To optimise resveratrol production, the effect of nutritional supplementation in the fermentation medium was analysed, considering a previous study that reported its influence on resveratrol titre and yield (Costa et al., 2022a). This earlier research indicated that resveratrol production by an engineered *S. cerevisiae* strain was 1.87 times higher when supplemented with 7.5 g/L of yeast extract compared to regular supplementation with yeast extract (10 g/L) and peptone (20 g/L) on YP medium (Costa et al., 2022a). Therefore, supplementation of different yeast extract concentrations (5, 7.5, 10, and 20 g/L) without peptone alongside regular YP supplementation as a control (yeast extract 10 g/L and peptone 20 g/L), was evaluated (Fig. 3). Here, the combination of yeast extract and peptone was more favourable for resveratrol production than the other conditions, as opposed to the results observed for *S. cerevisiae*. No significant differences were observed in resveratrol (Costa et al., 2022a) production between the different yeast extract concentrations tested. Moreover, reducing the concentration of yeast extract from 20 to 5 g/L led to decreased accumulation of *p*-coumaric acid (Fig. 3). As expected, biomass formation correlated with increased yeast extract supplementation. However, while resveratrol production is highly dependent on biomass, a balance between both seems necessary for increased yield, as an excessive allocation of carbon and nitrogen to biomass formation reduces the production of this metabolite (Costa et al., 2022a). The higher production of resveratrol using yeast extract and peptone supplementation observed here by *K. marxianus*, as opposed to *S. cerevisiae*, may be due to differences in the RBP pathway. In the phenylalanine pathway introduced into *S. cerevisiae* by Costa et al., 2022a, extra $NADP^+$ generated during the conversion of cinnamic acid to *p*-coumaric acid is reduced back to NAPDH to maintain intracellular redox balance. However, in the tyrosine pathway used in this work, this potential is not generated through the same way. Alternatively, it may be obtained from the metabolism of the additional amino acids present in peptone. In yeast, amino acids can be imported into the cell and converted into 2-oxo acid by aminotransferases, which can then be transformed into fusel aldehydes by 2-oxo acid decarboxylases. The conversion of fusel aldehydes into fusel acids by aldehyde dehydrogenases allows the regeneration of NAD(P)H (Hazelwood et al., 2008). One should not exclude the possibility that differences in nutrient requirements between these yeast could contribute to the observed differences in resveratrol production under the diverse conditions tested.

Raising the carbon content can enhance biomass formation, potentially benefiting resveratrol production. Given this, increasing glucose concentrations (36, 105, and 170 g/L) were used to assess their impact on resveratrol production. As anticipated, higher glucose concentrations led to increased resveratrol titres for both strains (Fig. 4A). This rise showed a linear correlation with the increase in biomass ($R^2 = 0.998$ for both strains). The higher concentration of resveratrol observed from YPD_{170} was associated with a lower accumulation of *p*-coumaric acid under this condition (Fig. 4B), indicating a more effective conversion of *p*-coumaric acid to resveratrol at the highest glucose concentration. Ethanol was only detected in the cultures with 170 g/L of glucose for both strains and it was consumed after 48 h (Table 1). Ethanol consumption may have contributed to the increased *p*-coumaric conversion to resveratrol under the YPD_{170} condition, as ethanol can be converted to acetyl-CoA, a precursor of malonyl-CoA, which combines with *p*-coumaroyl-CoA to produce resveratrol (Fig. 2A). Under the three conditions tested, no acetic acid was detected, suggesting its conversion to acetyl-CoA. Increasing glucose concentration led to higher glycerol production, with strain YBL001-RBP accumulating more glycerol than S9-RBP in all conditions. Specifically, for strain S9-RBP, there was a 98-fold increase from YPD_{170} compared to YPD_{36}, while for YBL001-RBP, a 36-fold increase was observed (Fig. 5). Despite *K. marxianus* being Crabtree-negative, meaning it typically does not exhibit ethanol fermentation under aerobic conditions, with increasing glucose concentration, some carbon was still diverted to produce primary metabolites, such as ethanol and glycerol. Glycerol accumulation during glucose metabolism occurs in response to redox imbalance, with glycerol production being accompanied by NADH generation to counteract this imbalance by regenerating NAD^+ (Zhang et al., 2020). These findings suggest that metabolic differences exist between the strains, although they may not always manifest as differences in resveratrol production.

3.3. Increased de novo resveratrol production from xylose and the positive effect of ethanol supplementation

Successful resveratrol production from xylose was previously reported in *S. cerevisiae* (Costa et al., 2022a). Given that *K. marxianus* can naturally metabolise xylose and this sugar is abundant in lignocellulosic hydrolysates, we aimed to produce resveratrol from xylose. This sugar is metabolised by *K. marxianus* into *D*-xylulose-5-phosphate, which enters the PPP, allowing the generation of E4P and glyceraldehyde-3-phosphate. The latest facilitates PEP formation, another precursor used in the shikimate pathway for resveratrol production (Fig. 2A) (Suástegui et al., 2017). Noteworthy, some authors reported an improved biosynthesis of acetyl-CoA-derived products when xylose is used as a carbon source compared to glucose due to the facilitated supply of acetyl-CoA in the cytosol (Kwak et al., 2017).

Resveratrol production at 48 h in YPX was 1.7-fold higher (p value $<$ 0.05) than in YPD_{36} for strain YBL001-RBP. Although it was not significantly higher for strain S9-RBP, a 1.4-fold increase in YPX compared to YPD_{36} was observed (Tables 1 and 2). Moreover, the yield of resveratrol per consumed sugar at 48 h was 1.8-fold higher (p value $<$ 0.05) for strain S9-RBP (0.44 ± 0.00 mg g^{-1}) and 2.1-fold higher (p value $<$ 0.05) for strain YBL001-RBP (0.48 ± 0.00 mg g^{-1}) in YPX compared to YPD_{36} (see Table 1 for YPD_{36} data). After 48 h of fermentation in YPD_{36}, strains S9-RBP and YBL001-RBP produced 9.94 ± 0.01 mg/L and 10.98 ± 0.08 mg/L of *p*-coumaric acid, respectively. In contrast, in YPX this metabolite was undetected at that time, indicating a

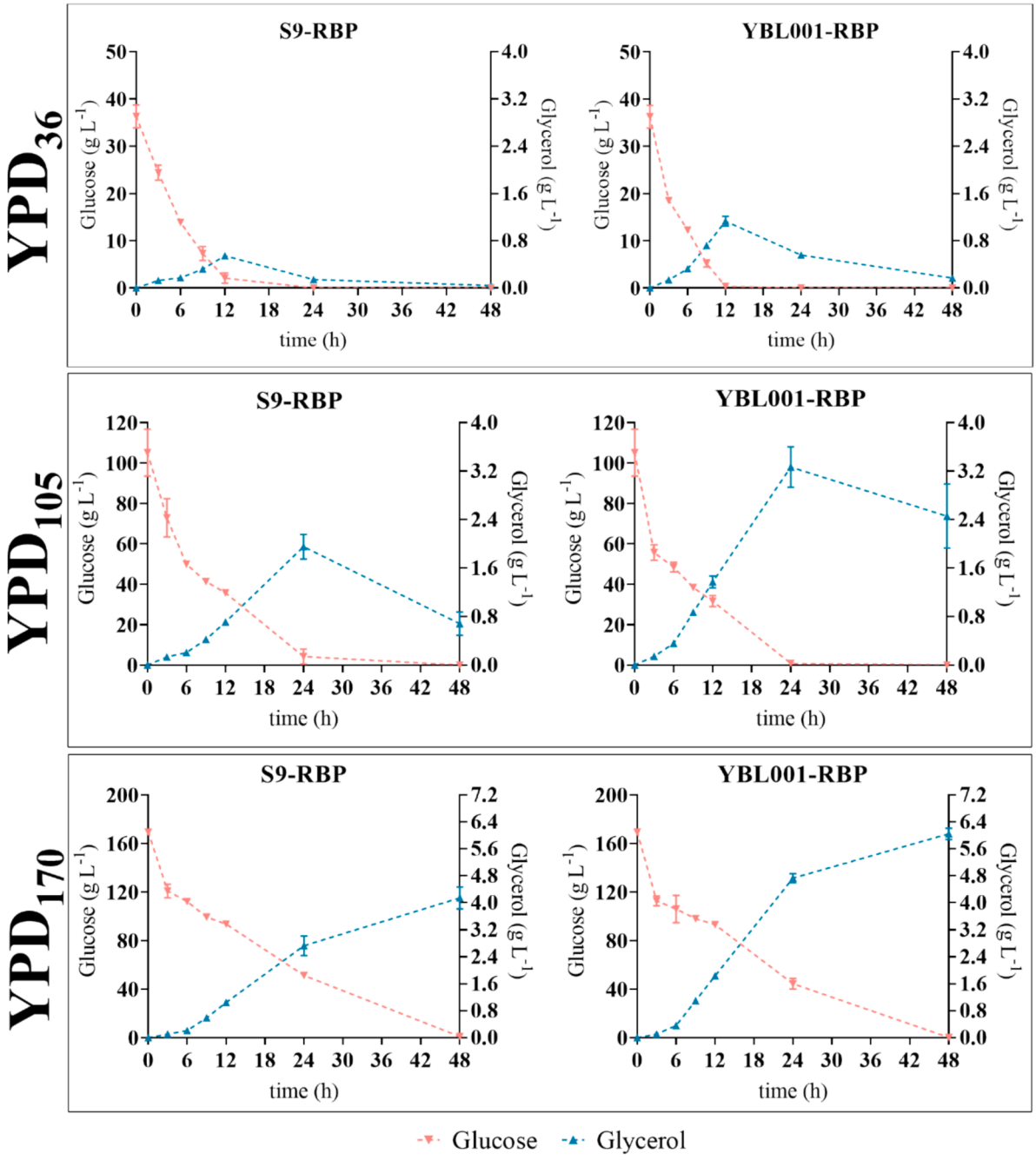

Fig. 5. Metabolites' profile of fermentations for resveratrol production with increasing glucose concentration. Fermentation profile of glucose (pink triangles) and glycerol (blue triangles) by the two engineered yeast expressing the resveratrol biosynthetic pathway (RBP), S9-RBP and YBL001-RBP, in baffled shake flasks in YPD medium with different glucose concentration (36, 105, and 170 g/L) at 30 ∘C, and 300 rpm. Each column represents the average values ± standard deviation of biological duplicates.

more efficient conversion to resveratrol. This suggests that xylose metabolism overcomes the limitation on acetyl-CoA observed under glucose metabolism. Ethanol can also act as a substrate for resveratrol *de novo* production and its supplementation is beneficial (Costa et al., 2021). Our results with the highest glucose concentration tested (170 g/L) indicated that ethanol consumption may have contributed to an increased acetyl-CoA supply, thereby enhancing resveratrol production (Table 1). Therefore, we tested the effect of supplementing 5 g/L of ethanol at 12 and 24 h in a xylose medium (Fig. 6). These time points were chosen because xylose metabolism was actively generating the *p*-coumaric acid precursor, and simultaneous ethanol consumption would provide sufficient acetyl-CoA for conversion to malonyl-CoA. Ethanol supplementation significantly increased resveratrol production and productivity. For strain S9-RBP, the resveratrol titre increased approximately 1.8-fold, from 12.57 ± 1.53 mg/L to 22.05 ± 2.30 mg/L. For strain YBL001-RBP, it increased 1.9-fold, from 10.88 ± 0.72 mg/L to 20.60 ± 0.50 mg/L (Fig. 6 and Table 2). The accumulation of *p*-coumaric acid was significantly higher without ethanol supplementation (2.1-fold for S9-RBP and 2.7-fold for YBL001-RBP) compared to YPX with ethanol supplementation. Biomass accumulation was also significantly higher with ethanol supplementation, 1.7-fold for S9-RBP and 1.8-fold for YBL001-RBP (Table 2), indicating that the assimilated ethanol also contributed to yeast growth. In fact, no significant differences were observed in the yield of resveratrol production per biomass dry cell

Table 2
Fermentation parameters of resveratrol production in xylose medium. Fermentation parameters of the recombinant strains expressing the resveratrol biosynthetic pathway (RBP) in two different host chassis (laboratory strain YBL001 and isolate from cocoa fermentation strain S9) in YPX and YPX with ethanol pulses at 12 and 24 h, at 30 ∘C.[a]

Strain	Condition	X_0 (g/L)	E_{48h} (g/L)	E_{96h} (g/L)	R_{48h} (mg/L)	R_{96h} (mg/L)	DCW-$_{96h}$ (g/L)	$Y_{R/DCW-96h}$ (mg g^{-1})	Q_{R-96h} (mg/Lh^{-1})	*p*-ca_{96h} (mg/L)
S9-RBP	YPX	28.80 ± 0.15	0.00 ± 0.00	0.00 ± 0.00	12.73 ± 0.06	12.57 ± 1.53	4.20 ± 0.10	2.99 ± 0.37	0.13 ± 0.02	13.94 ± 0.26
	YPX + EtOH	15.91 ± 0.15	2.74 ± 0.19	0.00 ± 0.00	11.12 ± 0.36	22.05 ± 2.30	7.20 ± 0.10	3.06 ± 0.32	0.23 ± 0.02	6.79 ± 0.11
YBL001-RBP	YPX	28.80 ± 0.15	0.00 ± 0.00	0.00 ± 0.00	13.65 ± 0.02	10.88 ± 0.72	4.90 ± 0.20	2.22 ± 0.15	0.11 ± 0.01	16.38 ± 0.11
	YPX + EtOH	15.91 ± 0.15	2.79 ± 0.03	0.00 ± 0.00	10.64 ± 0.00	20.60 ± 0.50	8.85 ± 0.45	2.33 ± 0.06	0.21 ± 0.01	6.13 ± 0.01

[a] X_0, initial xylose concentration; E_{48h}, ethanol concentration at 48 h; E_{96h}, final ethanol concentration at 96 h; R_{48h}, resveratrol concentration at 48 h; R_{96h}, resveratrol concentration in the end of fermentation (96 h); DCW-$_{96h}$, Dry Cell Weight in the end of fermentation (96 h); $Y_{R/DCW-96h}$, Yield of resveratrol per dry cell weight at 96 h; Q_{R-96h}, resveratrol productivity at 96 h; *p*-ca_{96h}, *p*-coumaric acid concentration in the end of fermentation (96 h).

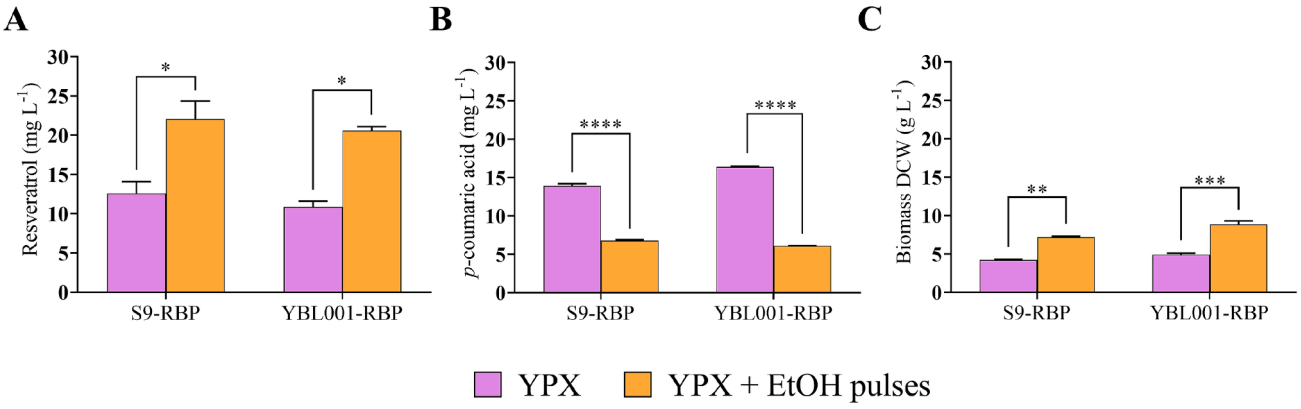

Fig. 6. Resveratrol production from xylose with or without ethanol supplementation. Resveratrol production (A), *p*-coumaric acid accumulation (B), and biomass dry cell weight (DCW; C) by the two engineered yeast expressing the resveratrol biosynthetic pathway (RBP), S9-RBP and YBL001-RBP, after 96 h of fermentation in baffled shake flasks in YPX medium (purple) and YPX with ethanol pulses (12 and 24 h) (orange) at 30 ∘C and 300 rpm. Each column represents the average values ± standard deviation of biological duplicates.

weight between YPX with or without ethanol for both strains.

Both strains consumed xylose after 48 h, and no glycerol, acetic acid, or ethanol were detected in YPX, regardless of ethanol supplementation. Strain S9-RBP produced 2.6 times more xylitol (3.12 ± 0.02 g/L) than YBL001-RBP (1.21 ± 0.03 g/L) after 24 h of fermentation in YPX without ethanol supplementation. Both strains consumed this sugar alcohol after 96 h. In YPX with ethanol supplementation, both strains produced significantly less xylitol (lower than 1 g/L), indicating that, with ethanol supplementation, the carbon from xylose metabolism was being directed towards biomass production rather than xylitol. Xylitol accumulation occurs due to a cofactor imbalance between xylose reductase and xylitol dehydrogenase (Lulu et al., 2013; Zhang et al., 2011). Since ethanol consumption leads to the regeneration of NADH, the reduced accumulation of xylitol in the cultures with ethanol supplementation could result from a reduced cofactor imbalance. The lower *p*-coumaric acid accumulation in the presence of ethanol might also have contributed to increased resveratrol production.

Alternative ethanol supplementation strategies should be explored to boost resveratrol yields, as ethanol consumption generates malonyl-CoA, a key co-precursor for resveratrol production. This approach could also reduce *p*-coumaric acid accumulation. Moreover, a multi-stage agitation strategy during culture may enhance resveratrol production, as shown in *S. cerevisiae* (Costa et al., 2022b). An initial 24-hour phase at 120 rpm could promote ethanol production, followed by increased agitation at 300 rpm for the remainder of the culture to facilitate ethanol consumption and thus, consequently, resveratrol synthesis.

3.4. Resveratrol production from the hemicellulosic hydrolysate and whole slurry by SSF of hydrothermally pretreated corn cob

Microbial production of resveratrol from lignocellulosic materials could have positive economic and environmental implications. Different lignocellulosic materials have been used for resveratrol production, such as vine pruning (Costa et al., 2022a) and *Eucalyptus globulus* wood (Costa et al., 2021). Considering that xylose is more favourable than glucose for resveratrol production (Tables 1 and 2) and this sugar can be obtained from xylan after hydrolysis, corn cob was chosen for resveratrol production given its high xylan content among other lignocellulosic materials. Additionally, the acetic acid present in the hydrolysate can be used for resveratrol production as it is converted to acetyl-CoA (Fig. 2A). Developing an integrated process for the complete valorisation of the corn cob biomass involves saccharifying the cellulose in the pretreated solid to release glucose. In an SSF, glucose released from the solid by cellulases mimics glucose supplementation in a fed-batch scheme, maintaining basal glucose levels and avoiding glucose repression on xylose when concentrations are high (Baptista et al., 2018). Noteworthy, the simultaneous consumption of glucose and xylose by *S. cerevisiae* (Costa et al., 2022a) favoured resveratrol production. Therefore, we hypothesised that an SSF process using the whole slurry of corn cob could also enhance resveratrol production by *K. marxianus*. Industrial strains are known to be more robust under stressful conditions, such as those faced during high-temperature fermentations of lignocellulosic materials. Strain S9-RBP was selected for these assays due to its thermotolerance and its ability to produce and consume ethanol under stress-intensive fermentation conditions (Baptista et al., 2021). Strain

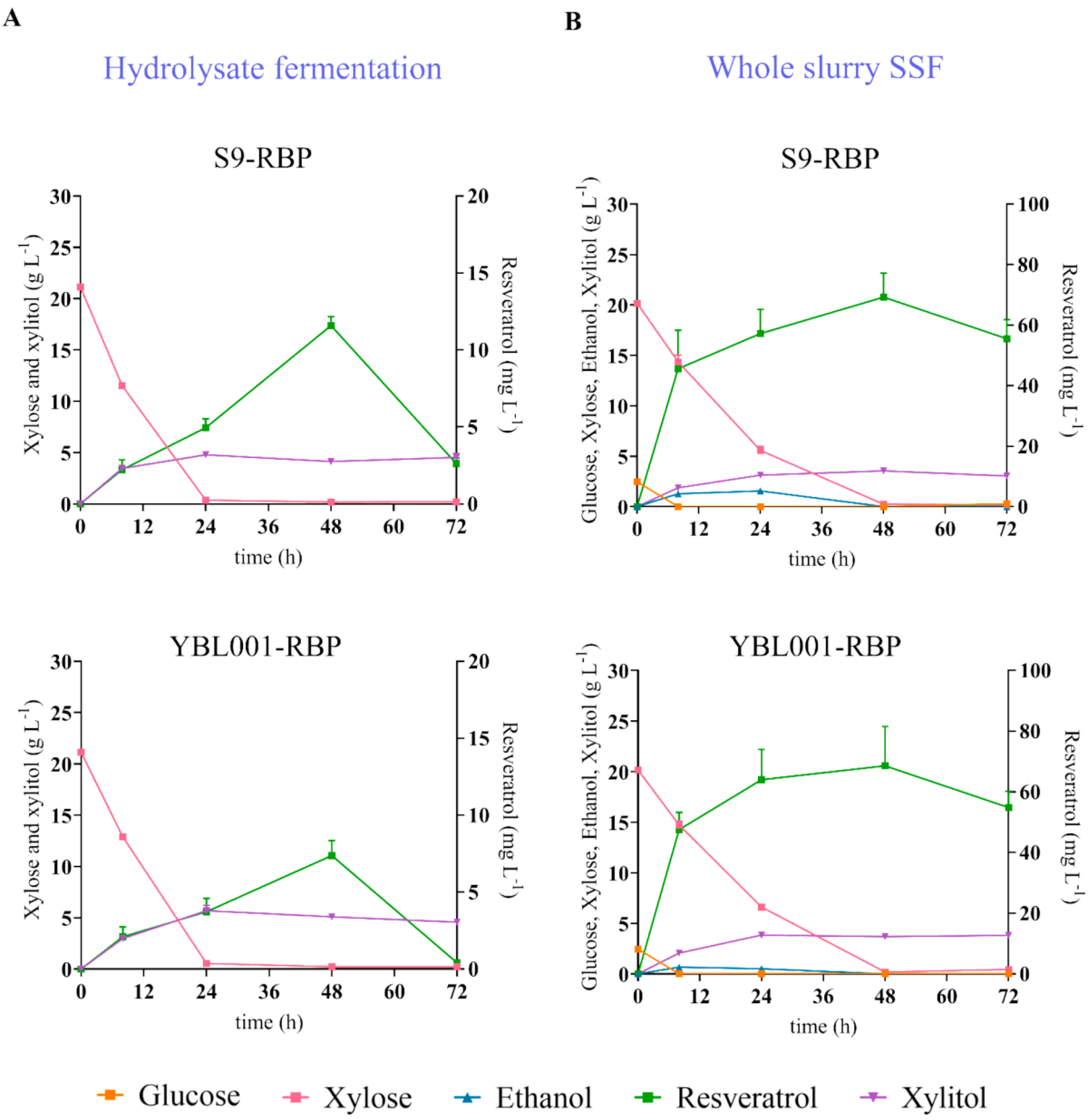

Fig. 7. Resveratrol production from corn cob. Fermentation profiles of produced metabolites and resveratrol from a corn cob hydrolysate (A) and whole slurry by SSF (B) by the recombinant strains expressing the resveratrol biosynthetic pathway (RBP), S9-RBP and YBL001-RBP, at 37 ∘C and 300 rpm. Glucose (orange squares); xylose (pink squares); ethanol (blue triangles); resveratrol (green squares); xylitol (purple triangles). Each data point represents the average ± standard deviation of biological duplicates.

Table 3
Fermentation parameters of resveratrol production from corn cob. Fermentation parameters of recombinant strains expressing the resveratrol biosynthetic pathway (RBP) in two different host chassis (laboratory strain YBL001 and isolate from cocoa fermentation strain S9) in a corn cob hydrolysate and whole slurry by SSF at 37 ∘C.[a]

Strain	X_0 (g/L)	G_0 (g/L)	GPOT (g/L)	X_{72h} (g/L)	E_{72h} (g/L)	R_{48h} (mg/L)	$XylOH_{72h}$ (g/L)	$Y_{R/S-48h}$ (mg g^{-1})	Q_{R-48h} (mg/Lh^{-1})
Corn cob hydrolysate									
S9-RBP	21.13 ± 0.01	1.70 ± 0.23	–	0.16 ± 0.01	0.00 ± 0.00	11.58 ± 0.41	4.66 ± 0.09	0.44 ± 0.02	0.24 ± 0.01
YBL001-RBP				0.19 ± 0.02	0.00 ± 0.00	7.38 ± 0.68	4.80 ± 0.14	0.28 ± 0.03	0.15 ± 0.01
Corn cob whole slurry									
S9-RBP	20.16 ± 0.22	2.47 ± 0.15	10.72 ± 3.75	0.20 ± 0.01	0.00 ± 0.00	69.26 ± 5.57	3.47 ± 0.31	–	1.44 ± 0.12
YBL001-RBP				0.76 ± 0.02	0.00 ± 0.00	68.61 ± 9.19	4.00 ± 0.14		1.43 ± 0.19

[a] X_0, initial xylose concentration; G_0, initial glucose concentration; G_{POT}, potential glucose to be obtained from the solid fraction (calculated according to (Costa et al., 2021)); X_{72h}, final xylose concentration (72 h); E_{72h}, final ethanol concentration (72 h); R_{48h}, maximum resveratrol concentration (48 h); $XylOH_{72h}$, final xylitol concentration (72 h); $Y_{R/S-48h}$, Yield of maximum resveratrol concentration per total sugars (glucose, xylose, and arabinose) consumed at 48 h; Q_{R-48h}, maximum resveratrol productivity (48 h).

Table 4
Microbial production of *p*-coumaric acid and resveratrol from yeast in synthetic medium and lignocellulosic feedstocks.

Product	Microorganism	Relevant genotype	Substrate	Titre (mg/L)	Yield on substrate (mg g^{-1})	Ref
p-coumaric acid	*S. cerevisiae*	*TAL* (*F. johnsoniae*)	Glucose	202 ± 0.005 [a]	1.00 + 0.00	(Rodriguez et al., 2017)
		TAL (*F. johnsoniae*), *aroL* (*E. coli*), *ARO7*fbr, *ARO4* fbr, Δ*ARO10*, Δ*PDC5* (*S. cerevisiae*)	Xylose	242 ± 12 [a]	9.68 ± 0.59	(Borja et al., 2019)
	K. marxianus	*TAL* (*F. johnsoniae*)	Glucose	31.12 ± 0.02[b]	1.50 ± 0.00	This study
			Xylose	20.08 ± 1.15[b]	1.07 ± 0.06	
Resveratrol	*S. cerevisiae*	*TAL* (*Herpetosiphon aurantiacus*), *4CL* (*A. thaliana*), *VST* (*V. vinifera*), *ARO4*fbr, *ARO7*fbr, Sc*ACC1*$^{S659A, S1157A}$ (*S. cerevisiae*)	Glucose, Ethanol	6.40 ± 0.03 [a]	0.02 ± 0.00 (on glucose) and 0.51 ± 0.01 (on ethanol)	(Li et al., 2015)
		PAL2, *4CL2*, *C4H*, *ATR2* (*A. thaliana*), *VST1* (*V. vinifera*)	*Eucalyptus globulus* wood[c]	151.65 ± 3.84	4.1 4 ± 0.11	(Costa et al., 2021)
		PAL2, *4CL2*, *C4H*, *ATR2* (*A. thaliana*), *VST1* (*V. vinifera*), *CYB5* (*S. cerevisiae*)*	Xylose, Glucose	388.4 ± 23.9[b]	6.5 ± 0.0	(Costa et al., 2022a)
			Vine pruning[d]	167.1 ± 9.8[b]	7.3 ± 0.4	
	S. stipitis	*TAL* (*H. aurantiacus*), *4CL2* (*A. thaliana*), *VST* (*V. vinifera*), *ARO7*fbr (*S. stipitis*)	Glucose	237.6[b]	4.75	(Kobayashi et al., 2021)
			Xylose	248.6[b]	4.97	
	Y. lypolytica	*TAL* (*Rhodotorula toruloides*), *4CL* (*Petroselinum crispum*), *VST* (*V. vinifera*), *ARO4*fbr (*S. cerevisiae*) *	Glucose	12.67 ± 2.23[b]	N.A.	(Gu et al., 2020)
	K. marxianus	*TAL* (*F. johnsoniae*), *4CL2* (*A. thaliana*), *VST* (*V. vinifera*)	Glucose	9.16 ± 1.60[b]	0.25 ± 0.04	This study
			Xylose	12.57 ± 1.53[b]	0.44 ± 0.00	
			Xylose, Ethanol	22.05 ± 2.30[b]	N.A.	
			Corn cob whole slurry[e]	69.26 ± 5.57[b]	N.A.	

*multiple modifications, refer to the original research article. N.A., not available. [a]batch bioreactor cultivations; [b]shake flask cultivations; [c]cellulosic fraction (glucose); [d]hemicellulosic fraction (mainly xylose); [e]cellulosic and hemicellulosic fractions (glucose + xylose).

YBL001-RBP was used as a control because of its capacity to grow at 37 ∘C and the widespread use of its parent strain (NBRC1777) in the literature. To evaluate the ability of the S9-RBP and YBL001-RBP strains to produce resveratrol from lignocellulosic materials, fermentation of the hemicellulosic hydrolysate (Fig. 7A) and SSF of the whole slurry (Fig. 7B) of pretreated corn cob were performed at 37 ∘C, leveraging the thermotolerance of *K. marxianus*. For SSF, 5 % solid loadings and 12 FPU/g of cellulase were used since these conditions were previously shown to facilitate efficient cellulose saccharification from corn cob while not limiting xylose uptake by yeast, thus reducing glucose repression on xylose consumption.

Both strains produced resveratrol from the corn cob hydrolysate, reaching peak production at 48 h. Strain YBL001-RBP produced 7.38 ± 0.68 mg/L, while strain S9-RBP achieved a 1.6-fold higher titre, reaching 11.58 ± 0.41 mg/L (Fig. 7A). Additionally, the yield of resveratrol per consumed sugars and the maximum productivity at 48 h for strain S9-RBP from the corn cob hydrolysate were 1.6-fold significantly higher than those of YBL001-RBP (p value < 0.05) (Table 3). Notably, no acetic acid or glycerol was detected after 72 h, indicating that xylose was being assimilated through the PPP.

Fermentation of the whole slurry via SSF yielded higher resveratrol titres after 48 h compared to corn cob hydrolysate for both strains. Strain S9-RBP produced 69.26 ± 5.57 mg/L, while strain YBL001-RBP reached 68.61 ± 9.19 mg/L, marking an approximately 6.0-fold increase for strain S9-RBP and a 9.3-fold increase for strain YBL001-RBP (Fig. 7B), attributed to the higher carbon content. The maximum productivity of resveratrol from the whole slurry was the highest obtained in this work for both strains (S9-RBP − 1.44 ± 0.12 mg/Lh^{-1}; YBL001-RBP −1.43 ± 0.19 mg/Lh^{-1}) (Table 3). After 72 h of whole slurry fermentation, no ethanol, acetic acid, or glycerol were detected, although strain S9-RBP initially produced a higher concentration of ethanol during the process (Table 3). The high resveratrol concentration achieved by both strains from the SSF of the whole slurry, coupled with the absence of xylose accumulation at the end of the fermentation, indicates that xylose uptake remained uncompromised during glucose release from the cellulosic fraction, suggesting that the SSF conditions were suitable.

Resveratrol degradation after 72 h was observed for both fermentations, probably due to the observed rise in pH from 5.5 to 8. Such an increase is known to adversely affect the stability of *trans*-resveratrol (Robinson et al., 2015). Also, the high fermentation temperature may have had a synergistic effect contributing to the instability of resveratrol. However, it is worth noting that the maximum concentration of resveratrol was attained at 48 h, allowing the cultures to be halted before this degradation issue becomes significant.

Xylitol accumulation was 1.3-fold higher from the corn cob hydrolysate compared to the whole slurry for strain S9-RBP (4.66 ± 0.09 g/L from the hydrolysate and 3.47 ± 0.31 g/L from the whole slurry) and 1.2-fold for strain YBL001-RBP (4.80 ± 0.14 and 4.00 ± 0.14 g/L, respectively) (Table 3). The greater accumulation of xylitol from the corn cob hydrolysate, where xylose is the primary carbon source, compared to the whole slurry SSF, where glucose is released from the cellulosic fraction, may be attributed to a cofactor imbalance. Xylose reduction to xylitol by xylose reductase requires NADPH. In the presence of glucose, less NADPH may be available for this reaction, limiting xylitol accumulation. Conversely, glucose metabolism via glycolysis generates NADH, which is not utilised in the xylose-to-xylitol conversion.

Both strains depleted xylose from the hydrolysate within 24 h, a process 24 h faster than observed in the synthetic medium at 30 ∘C. Transcriptional analysis of *K. marxianus* cells indicated upregulation of the PPP at higher temperatures (Li et al., 2019), possibly explaining the faster xylose consumption at 37 ∘C compared to 30 ∘C. In the SSF of the whole slurry, complete xylose consumption was observed only after 48 h, with glucose undetectable at the end of the fermentation. This delay, compared to the fermentation of the hydrolysate, is attributed to the simultaneous release of glucose from the solid fraction.

In the fermentation with the corn cob hydrolysate, there was no observed accumulation of *p*-coumaric acid, indicating that the xylose metabolism through the PPP favoured resveratrol production by fully converting *p*-coumaric acid.

However, in the fermentation of the whole slurry, after 48 h, strain YBL001-RBP accumulated approximately 1.3-fold more *p*-coumaric acid (10.38 ± 2.02 mg/L) than S9-RBP (7.69 ± 0.88 mg/L). By 72 h, the *p*-coumaric acid concentration increased approximately 3.5 times for strain YBL001-RBP (34.79 ± 0.62 mg/L) and 4 times for strain S9-RBP (32.52 ± 1.76 mg/L) compared to 48 h. The accumulation of *p*-coumaric acid in the whole slurry but not in the hydrolysate results from glucose metabolism and the higher carbon content. Ethanol depletion after 48 h from the fermentation of the whole slurry was accompanied by *p*-coumaric acid accumulation at this time point, a phenomenon previously observed in *S. cerevisiae* (Costa et al., 2022a).

For a comparison of the *p*-coumaric acid and resveratrol titres and yield on substrate obtained in this work and others in the literature refer to Table 4. It is important to note that while our results represent a significant advancement in resveratrol production by *K. marxianus*, moving towards an integrated process using lignocellulosic materials, several challenges may arise during scale-up. These challenges include: i) resveratrol stability, which is influenced by factors such as dissolved oxygen, pH, temperature and light, all of which must be carefully monitored; ii) *p*-coumaric acid accumulation, which might be controlled by the adoption of metabolic engineering strategies, but remains a concern due to its proven toxicity to yeast cells (Mao et al., 2023); and iii) maintaining adequate oxygenation levels, as resveratrol production is oxygen-dependent.").

4. Conclusions

For the first time, the ability of *K. marxianus* strains to produce *p*-coumaric acid and resveratrol from glucose, xylose, and/or ethanol has been demonstrated. Xylose facilitates acetyl-CoA supply, while ethanol supplementation in xylose limits xylitol accumulation. To further reduce *p*-coumaric acid accumulation, different ethanol supplementation strategies warrant exploration. Potential enhancements include augmenting *p*-coumaric acid conversion yield, alleviating feedback inhibition in the shikimate pathway to prevent *p*-coumaric acid accumulation and/or the integration of multiple copies of the RBP. This study showcases the complete utilisation of corn cob for resveratrol production, a significant stride in advancing biorefineries and fostering circular bioeconomies.

CRediT authorship contribution statement

Marlene Baptista: Writing – original draft, Visualization, Methodology, Investigation, Formal analysis, Conceptualization. **Carlos E. Costa:** Writing – review & editing, Visualization, Validation, Supervision, Methodology, Conceptualization. **Lucília Domingues:** Writing – review & editing, Validation, Supervision, Resources, Project administration, Methodology, Funding acquisition, Conceptualization.

Declaration of competing interest

The authors declare that they have no known competing financial interests or personal relationships that could have appeared to influence the work reported in this paper.

Acknowledgments

This work was funded by the Portuguese Foundation for Science and Technology (FCT) under the scope of the strategic funding of UIDB/04469/2020 unit with DOI 10.54499/UIDB/04469/2020, and Marlene Baptista PhD scholarship with DOI 10.54499/2020.06888.BD. Carlos E. Costa acknowledges the FCT through the ESSEntial project (PTDC/BII-BTI/1858/2021). Special thanks to Dr. Jean-Marc Daran from the Faculty of Applied Sciences of TU Delft for providing some parts from the YTK *Kluyveromyces* kit (plasmids containing the promoters and terminators used) and plasmids pGGKd015, pGGKd072 and pGGKd068.

E-supplementary data of this word can be found in online version of the paper.

Appendix A. Supplementary data

Supplementary data to this article can be found online at https://doi.org/10.1016/j.biortech.2024.131755.

Data availability

Data will be made available on request.

References

Baptista, S.L., Cunha, J.T., Romaní, A., Domingues, L., 2018. Xylitol production from lignocellulosic whole slurry corn cob by engineered industrial *Saccharomyces cerevisiae* PE-2. Bioresour. Technol. 267, 481–491. https://doi.org/10.1016/j.biortech.2018.07.068.

Baptista, M., Cunha, J.T., Domingues, L., 2021. Establishment of *Kluyveromyces marxianus* as a microbial cell factory for lignocellulosic processes: production of high value furan derivatives. J. Fungi 7, 1047. https://doi.org/10.3390/jof7121047.

Baptista, M., Domingues, L., 2022. *Kluyveromyces marxianus* as a microbial cell factory for lignocellulosic biomass valorisation. Biotechnol. Adv. 60, 108027. https://doi.org/10.1016/j.biotechadv.2022.108027.

Borja, G.M., Rodriguez, A., Campbell, K., Borodina, I., Chen, Y., Nielsen, J., 2019. Metabolic engineering and transcriptomic analysis of *Saccharomyces cerevisiae* producing p-coumaric acid from xylose. Microb. Cell Fact. 18. https://doi.org/10.1186/s12934-019-1244-4.

Costa, C.E., Romaní, A., Cunha, J.T., Johansson, B., Domingues, L., 2017. Integrated approach for selecting efficient *Saccharomyces cerevisiae* for industrial lignocellulosic fermentations: importance of yeast chassis linked to process conditions. Bioresour. Technol. 227, 24–34. https://doi.org/10.1016/j.biortech.2016.12.016.

Costa, C.E., Møller-Hansen, I., Romaní, A., Teixeira, J.A., Borodina, I., Domingues, L., 2021. Resveratrol production from hydrothermally pretreated eucalyptus wood using recombinant industrial *Saccharomyces cerevisiae* strains. ACS Synth. Biol. 10, 1895–1903. https://doi.org/10.1021/acssynbio.1c00120.

Costa, C.E., Romaní, A., Møller-Hansen, I., Teixeira, J.A., Borodina, I., Domingues, L., 2022a. Valorisation of wine wastes by de novo biosynthesis of resveratrol using a recombinant xylose-consuming industrial *Saccharomyces cerevisiae* strain. Green Chem. 24, 9128–9142. https://doi.org/10.1039/d2gc02429b.

Costa, C.E., Romaní, A., Teixeira, J.A., Domingues, L., 2022b. Resveratrol production for the valorisation of lactose-rich wastes by engineered industrial *Saccharomyces cerevisiae*. Bioresour. Technol. 359. https://doi.org/10.1016/j.biortech.2022.127463.

Costa, C.E., Romaní, A., Domingues, L., 2024. Overview of resveratrol properties, applications, and advances in microbial precision fermentation. Crit Rev Biotech. in press. https://doi.org/10.1080/07388551.2024.2424362.

De La Lastra, C.A., Villegas, I., 2005. Resveratrol as an anti-inflammatory and anti-aging agent: mechanisms and clinical implications. Mol. Nutr. Food Res. 49, 405–430. https://doi.org/10.1002/mnfr.200500022.

Dekker, W.J.C., Ortiz-Merino, R.A., Kaljouw, A., Battjes, J., Wiering, F.W., Mooiman, C., de la Torre, P., Pronk, J.T., 2021. Engineering the thermotolerant industrial yeast *Kluyveromyces marxianus* for anaerobic growth. Metab. Eng. 67, 347–364. https://doi.org/10.1016/j.ymben.2021.07.006.

del Río, P.G., Domínguez, E., Domínguez, V.D., Romaní, A., Domingues, L., Garrote, G., 2019. Third generation bioethanol from invasive macroalgae *Sargassum muticum* using autohydrolysis pretreatment as first step of a biorefinery. Renew. Energy 141, 728–735. https://doi.org/10.1016/j.renene.2019.03.083.

Donnez, D., Jeandet, P., Clément, C., Courot, E., 2009. Bioproduction of resveratrol and stilbene derivatives by plant cells and microorganisms. Trends Biotechnol. 27, 706–713. https://doi.org/10.1016/j.tibtech.2009.09.005.

Furukawa, K., Heinzle, E., Dunn, I.J., 1983. Influence of oxygen on the growth of *Saccharomyces cerevisiae* in continuous culture. Biotechnol. Bioeng. 25, 2293–2317. https://doi.org/10.1002/bit.260251003.

Gandam, K.P., Chinta, L.M., Gandham, P.A., Pabbathi, P.P.N., Konakanchi, S., Bhavanam, A., Atchuta, R.S., Baadhe, R.R., Bhatia, K.R., 2022. A New Insight into the Composition and Physical Characteristics of Corncob-Substantiating Its Potential for Tailored Biorefinery Objectives. https://doi.org/10.3390/fermentation.

Ghose, T.K., 1987. Measurement of cellulase activities. Pure Appl. Chem. 59, 257–268.

Gietz, R.D., 2014. Yeast Transformation by the LiAc / SS Carrier. In: Smith, J.S., Burke, D.J. (Eds.), Yeast Genetics: Methods and Protocols. Springer Science+ Business Media, New York, pp. 33–44. https://doi.org/10.1007/978-1-4939-1363-3.

Gu, Y., Ma, J., Zhu, Y., Ding, X., Xu, P., 2020. Engineering *Yarrowia lipolytica* as a chassis for de novo synthesis of five aromatic-derived natural products and chemicals. ACS Synth. Biol. 9, 2096–2106. https://doi.org/10.1021/acssynbio.0c00185.

Hassing, E.J., de Groot, P.A., Marquenie, V.R., Pronk, J.T., Daran, J.M.G., 2019. Connecting central carbon and aromatic amino acid metabolisms to improve de novo

2-phenylethanol production in *Saccharomyces cerevisiae*. Metab. Eng. 56, 165–180. https://doi.org/10.1016/j.ymben.2019.09.011.
Hassing, E.J., Buijs, J., Blankerts, N., Luttik, M.A., de Hulster, E.A., Pronk, J.T., Daran, J. M., 2021. Elimination of aromatic fusel alcohols as by-products of *Saccharomyces cerevisiae* strains engineered for phenylpropanoid production by 2-oxo-acid decarboxylase replacement. Metab. Eng. Commun. 13, e00183.
Hazelwood, L.A., Daran, J.-M., van Maris, A.J.A., Pronk, J.T., Dickinson, J.R., 2008. The Ehrlich pathway for fusel alcohol production: A century of research on *Saccharomyces cerevisiae* metabolism. Appl. Environ. Microbiol. 74, 2259–2266. https://doi.org/10.1128/AEM.02625-07.
Kang, S.Y., Lee, J.K., Choi, O., Kim, C.Y., Jang, J.H., Hwang, B.Y., Hong, Y.S., 2014. Biosynthesis of methylated resveratrol analogs through the construction of an artificial biosynthetic pathway in *E. coli*. BMC Biotech. 14. https://doi.org/10.1186/1472-6750-14-67.
Karim, A., Gerliani, N., Aïder, M., 2020. *Kluyveromyces marxianus*: an emerging yeast cell factory for applications in food and biotechnology. Int. J. Food Microbiol. 333, 108818. https://doi.org/10.1016/j.ijfoodmicro.2020.108818.
Kobayashi, Y., Inokuma, K., Matsuda, M., Kondo, A., Hasunuma, T., 2021. Resveratrol production from several types of saccharide sources by a recombinant *Scheffersomyces stipitis* strain. Metab. Eng. Commun. 13, e00188.
Kwak, S., Kim, S.R., Xu, H., Zhang, G.C., Lane, S., Kim, H., Jin, Y.S., 2017. Enhanced isoprenoid production from xylose by engineered *Saccharomyces cerevisiae*. Biotechnol. Bioeng. 114, 2581–2591. https://doi.org/10.1002/bit.26369.
Lane, M.M., Morrissey, J.P., 2010. *Kluyveromyces marxianus*: a yeast emerging from its sister's shadow. Fungal Biol. Rev. 24, 17–26. https://doi.org/10.1016/j.fbr.2010.01.001.
Lee, M.E., DeLoache, W.C., Cervantes, B., Dueber, J.E., 2015. A highly characterized yeast toolkit for modular, multipart assembly. ACS Synth. Biol. 4, 975–986. https://doi.org/10.1021/sb500366v.
Li, P., Fu, X., Chen, M., Zhang, L., Li, S., 2019. Proteomic profiling and integrated analysis with transcriptomic data bring new insights in the stress responses of *Kluyveromyces marxianus* after an arrest during high-temperature ethanol fermentation. Biotechnol. Biofuels 12, 1–13. https://doi.org/10.1186/s13068-019-1390-2.
Li, M., Kildegaard, K.R., Chen, Y., Rodriguez, A., Borodina, I., Nielsen, J., 2015. *De novo* production of resveratrol from glucose or ethanol by engineered *Saccharomyces cerevisiae*. Metab. Eng. 32, 1–11. https://doi.org/10.1016/j.ymben.2015.08.007.
Li, M., Schneider, K., Kristensen, M., Borodina, I., Nielsen, J., 2016. Engineering yeast for high-level production of stilbenoid antioxidants. Sci. Rep. 6, 1–8. https://doi.org/10.1038/srep36827.
Li, M., Lang, X., Moran Cabrera, M., De Keyser, S., Sun, X., Da Silva, N., Wheeldon, I., 2021. CRISPR-mediated multigene integration enables Shikimate pathway refactoring for enhanced 2-phenylethanol biosynthesis in *Kluyveromyces marxianus*. Biotechnol. Biofuels 14, 1–15. https://doi.org/10.1186/s13068-020-01852-3.
Lulu, L., Ling, Z., Dongmei, W., Xiaolian, G., Hisanori, T., Hidehiko, K., Jiong, H., 2013. Identification of a xylitol dehydrogenase gene from *Kluyveromyces marxianus* NBRC1777. Mol. Biotechnol. 53, 159–169. https://doi.org/10.1007/s12033-012-9508-9.
Madeira-Jr, J.V., Gombert, A.K., 2018. Towards high-temperature fuel ethanol production using *Kluyveromyces marxianus*: On the search for plug-in strains for the Brazilian sugarcane-based biorefinery. Biomass Bioenergy 119, 217–228. https://doi.org/10.1016/j.biombioe.2018.09.010.
Mao, J., Mohedano, M.T., Fu, J., Li, X., Liu, Q., Nielsen, J., Siewers, V., Chen, Y., 2023. Fine-tuning of p-coumaric acid synthesis to increase (2S)-naringenin production in yeast. Metab. Eng. 79, 192–202. https://doi.org/10.1016/j.ymben.2023.08.003.
Pereira, M., Schwan, R., Teixeira, J., 1999. Isolation, Screening, and Characterisation of Flocculating and Pectinase Producing *Kluyveromyces* Strains. Food Technol. Biotechnol. 37, 257–261.
Rajkumar, A.S., Morrissey, J.P., 2020. Rational engineering of *Kluyveromyces marxianus* to create a chassis for the production of aromatic products. Microb. Cell Fact. 19, 1–19. https://doi.org/10.1186/s12934-020-01461-7.
Rajkumar, A.S., Varela, J.A., Juergens, H., Daran, J.-M.-G., Morrissey, J.P., 2019. Biological parts for *Kluyveromyces marxianus* synthetic biology. Front. Bioeng. Biotechnol. 7, 1–15. https://doi.org/10.3389/fbioe.2019.00097.
Rivas, B., Torre, P., Dominguez, J.M., Converti, A., Parajo, J.C., 2006. Purification of xylitol obtained by fermentation of corncob hydrolysates. J. Agric. Food Chem. 54, 4430–4435. https://doi.org/10.1021/jf053156x.
Robinson, K., Mock, C., Liang, D., 2015. Pre-formulation studies of resveratrol. Drug Dev. Ind. Pharm. 41, 1464–1469. https://doi.org/10.3109/03639045.2014.958753.
Rodriguez, A., Chen, Y., Khoomrung, S., Özdemir, E., Borodina, I., Nielsen, J., 2017. Comparison of the metabolic response to over-production of p-coumaric acid in two yeast strains. Metab. Eng. 44, 265–272. https://doi.org/10.1016/j.ymben.2017.10.013.
Sáez-Sáez, J., Wang, G., Marella, E.R., Sudarsan, S., Cernuda Pastor, M., Borodina, I., 2020. Engineering the oleaginous yeast *Yarrowia lipolytica* for high-level resveratrol production. Metab. Eng. 62, 51–61. https://doi.org/10.1016/j.ymben.2020.08.009.
Sakihama, Y., Hidese, R., Hasunuma, T., Kondo, A., 2019. Increased flux in acetyl-CoA synthetic pathway and TCA cycle of *Kluyveromyces marxianus* under respiratory conditions. Sci. Rep. 9, 1–7. https://doi.org/10.1038/s41598-019-41863-1.
Shafiei-Alavijeh, R., Aghbashlo, M., Tabatabaei, M., Denayer, J.F.M., Karimi, K., 2024. A critical review of sustainable biorefineries utilizing high-solid processing for industrial crop lignocellulosic wastes valorization. Ind. Crop. Prod. 211, 118236. https://doi.org/10.1016/j.indcrop.2024.118236.
Solladié, G., Pasturel-Jacope, Y., Maignan, J., 2003. A re-investigation of resveratrol synthesis by Perkins reaction. Application to the synthesis of aryl cinnamic acids. Tetrahedron 59, 3315–3321. https://doi.org/10.1016/S0040-4020(03)00405-8.
Suástegui, M., Yu Ng, C., Chowdhury, A., Sun, W., Cao, M., House, E., Maranas, C.D., Shao, Z., 2017. Multilevel engineering of the upstream module of aromatic amino acid biosynthesis in *Saccharomyces cerevisiae* for high production of polymer and drug precursors. Metab. Eng. 42, 134–144. https://doi.org/10.1016/j.ymben.2017.06.008.
Vos, T., Cortés, P. de la T., Gulik, W.M. van, Pronk, J.T., Daran-Lapujade, P., 2015. Growth-rate dependency of de novo resveratrol production in chemostat cultures of an engineered *Saccharomyces cerevisiae* strain. Microb. Cell Fact. 14. https://doi.org/10.1186/s12934-015-0321-6.
Weber, E., Engler, C., Gruetzner, R., Werner, S., Marillonnet, S., 2011. A modular cloning system for standardized assembly of multigene constructs. PLoS One 6, e16765.
Zhang, B., Zhang, L., Wang, D., Gao, X., Hong, J., 2011. Identification of a xylose reductase gene in the xylose metabolic pathway of *Kluyveromyces marxianus* NBRC1777. J. Ind. Microbiol. Biotechnol. 38, 2001–2010. https://doi.org/10.1007/s10295-011-0990-z.
Zhang, B., Ren, L., Wang, Y., Xu, D., Zhang, S., Wang, H., Wang, H., Zeng, X., Xin, B., Li, F., 2020. Glycerol production through TPI1 defective *Kluyveromyces marxianus* at high temperature with glucose, fructose, and xylose as feedstock. Biochem. Eng. J. 161, 107689. https://doi.org/10.1016/j.bej.2020.107689.